Observation of Spatially Localized Atomic Electron Wave Packets

John A. Yeazell and C. R. Stroud, Jr.
The Institute of Optics, The University of Rochester, Rochester, New York 14627
(Received 21 January 1988)

We have excited and detected an atomic electron wave packet that is localized in the polar and azimuthal angles. The wave packet is formed through the coherent superposition of Rydberg states of atomic sodium. The superposition is achieved by short-pulse optical excitation of the atom in the presence of a strong rf field. The wave packet is detected by dc field ionization. The behavior of this wave packet in a strong dc field is much different from that of an eigenstate. This behavior agrees well with a simple classical model.

PACS numbers: 32.90.+a, 31.50.+w, 32.60.+i

Several recent papers[1-5] have discussed the possibility of forming a localized wave packet through the coherent superposition of atomic Rydberg states. The study of atomic coherent states began[6] shortly after the development of quantum mechanics and the theoretical treatment of these states has been extensive.[6-10] The fundamental concern of these studies is to understand the transition between classical and quantum physics. Recently, the interest in these states has increased because of the development of short-pulse lasers. The large coherent bandwidth of these pulses makes it likely that the result of this field acting upon an atom is best described in terms of atomic coherent states. In our previous paper[4] we proposed the excitation of a Rydberg atomic wave packet localized in two of the spherical coordinates, the polar and azimuthal angles. Here we report the observation of such a wave packet and examine its behavior in a strong dc field. This behavior agrees well with a simple classical model.

The wave packet is formed in the high-angular-momentum Rydberg states of atomic sodium. The advantages of the use of such states are several, as has been demonstrated by the recent experiment on inhibited spontaneous emission.[11] The chief advantage, for this experiment, is the possibility of our obtaining a nearly uniform energy spacing between the excited eigenstates. This reduces the rate at which the wave packet disperses. Another feature is the exceedingly large electric dipole matrix elements that exist between neighboring states: A modest rf field is sufficient to dress strongly states with the same principal quantum number. This dressing plays a critical role in the excitation of the wave packet.

The excitation of the angularly localized wave packet is achieved through the optical excitation of Rydberg states that are being strongly dressed by an rf field. A circularly polarized optical field is tuned to the two-photon resonance between the ground state and the $n=50$ (principal quantum number) manifold of states. This manifold of states is being strongly dressed by a circularly polarized rf field, tuned near the thirty-photon resonance between the $50d$ state and the $l=32$ state. This high-angular-momentum state and several of its neighbors are strongly mixed with the $50d$ state. All of these rf-dressed states lie within the coherent bandwidth of the optical pulse and can be excited by it. Following an adiabatic turnoff of the rf field, the population in the dressed states goes directly into the eigenstates with which they are linked. So we are left with a coherent superposition of high-angular-momentum eigenstates. The details of this excitation have been discussed more fully in our previous paper.[4] Figure 1(a) shows the wave packet which results from a numerical model of this excitation scheme. For comparison, Fig. 1(b) shows a high-angular-momentum eigenstate. The initial orientation of the wave packet lies along the direction of the rf-field vector at the time of the optical excitation. The optical pulse is short compared with the period of the motion of the rf-field vector. After the rf field is turned off, the motion of the wave packet is due to the core polarization of the sodium atom. This motion agrees with the precession of a classical orbit perturbed by an r^{-4} potential.[4] It should be noted that the motion and rate of dispersion of the wave packet are very slow (of order milliseconds).

The ionization of the angularly localized wave packet, due to a pulsed electric field, occurs differently from the ionization of an eigenstate. Classical calculations have proven highly successful in modeling the response of weakly bound states to the influence of an electric field.[12-16] We have formulated a classical Monte Carlo-type model to describe the ionization of the wave packet. The initial state is formed by selection of a set of classical trajectories which have an average energy, an average angular momentum, and a probability distribution in agreement with that of the angular wave packet. These trajectories are then allowed to evolve under the influence of a pulsed ionizing electric field. The resulting ionization signal depends both on time and on the angular localization of the wave packet. Figure 2 shows the ionization signal as a function of time. The three curves

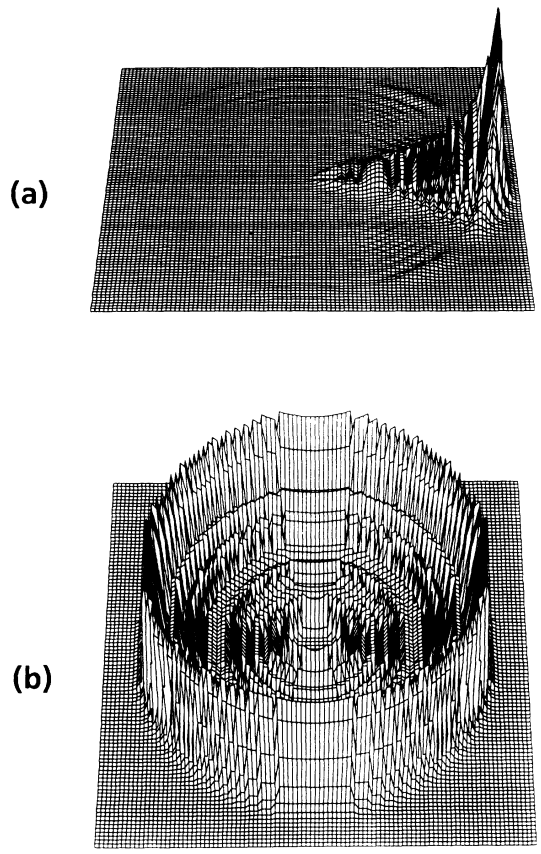

FIG. 1. (a) The probability distribution of the angularly localized wave packet, in the x-y plane, in the form of a 3D plot. Since the wave packet is formed from high-angular-momentum states ($n=50$, $29<l<37$, $m=l$), the probability of the wave packet being found outside of the x-y plane is small. The orientation of the wave packet is along the direction of the rf field vector. The peak of the distribution occurs at 5000 Bohr radii. The parameters used in the numerical model agree with the experimental conditions. (b) The probability distribution of an eigenstate ($n=50$, $l=32$, $m=32$) for comparison.

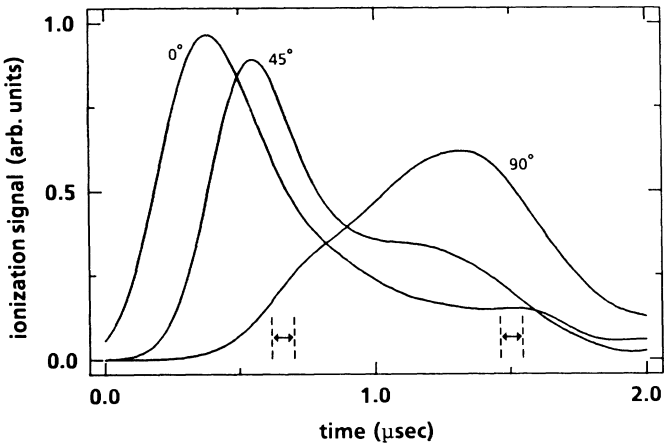

FIG. 2. The ionization signals from three angular wave packets (20° FWHM) as functions of time. The time dependence of the ionization signal depends on the orientation of the wave packet with respect to the ionizing field. The origin of the time axis is 50 μsec after the ionization pulse (the transit time to the detector has been suppressed). The hash marks indicate the widths and positions of the boxcar window for the results shown in Figs. 4 and 5.

correspond to angular wave packets which differ only in their orientations with respect to the ionizing field. A wave packet aligned with the ionizing field (0°) has a greater ionization rate than one aligned in another direction. It should be noted that in a typical experiment, any wave packet, regardless of orientation, will be ionized. This means that the total ion yield will not show an angular dependence. However, the ionization signal, at a given time, depends strongly on the orientation of the wave packet. For example, at 1.5 μsec, wave packets oriented at 90° to the ionizing field dominate.

Figure 3 shows the apparatus used to excite and detect the wave packet. A dense sodium atomic beam ($\simeq 10^9/\text{cm}^3$), 1 mm in diameter, enters the interaction region. The optical excitation occurs at the center of this region where the rf antenna has produced a circularly polarized field with an amplitude of 0.3 V/cm and frequency of 65 MHz. The optical pulse is produced by an excimer-pumped dye laser (coumarin 480, 4837 Å). The excimer laser (XeCl) produces a pump pulse that is 3 nsec in duration and has an energy of 60 mJ. This drives the dye oscillator far above threshold, resulting in a shorter pulse than usual for a Hänsch type of laser (FWHM = 500 psec). The frequency bandwidth of this pulse is 0.05 cm^{-1}, which is approximately 1.5 times the transform limit for this pulse shape. The bandwidth should overlap about ten dressed states. The optical field is converted to circular polarization before entering the interaction region. Following the optical excitation, the rf field is turned off adiabatically over a span of 5 μsec. A transient digitizer (Tektronics 7912AD) is triggered by the optical pulse in order to obtain a measurement of

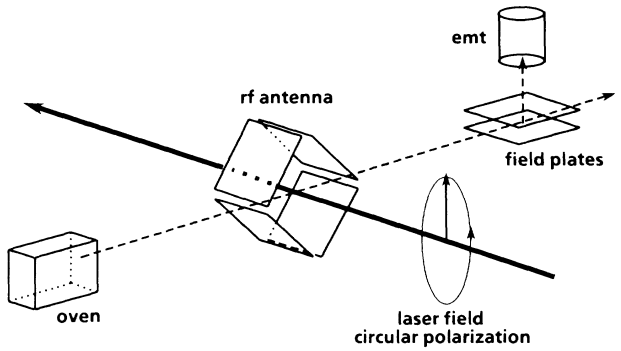

FIG. 3. Scheme of the experimental setup.

the phase of the rf field relative to the optical pulse. This is necessary to determine the direction of localization of the wave packet. The excited atoms leave the interaction region and enter the region in which they will be ionized. A short electrical pulse (10 nsec, 200 V/cm), synchronized to the optical pulse, is applied to the ionization plates. After the ionization pulse, the ions travel in a field-free region which spreads out the ion signal in time. The ions are then accelerated into an electron multiplier and the output signal is fed to a boxcar integrator. The boxcar window examines only a small portion ($\simeq \frac{1}{30}$) of the time-resolved ion signal. The result of each laser shot must be correlated with the phase of the rf field, so that no averaging takes place within the boxcar. The output of the boxcar is recorded by a microcomputer and combined with the phase information, so that data with the same relative phase are averaged.

The ionization signal depends on both the position of the boxcar window (time) and the direction in which the wave packet is localized. The beginning of the ion signal is obscured by photoions produced by direct three-photon ionization from the ground state. However, by movement of the window more toward the center of the ion signal, the photoion-induced noise disappears. Here, the ion yield exhibits a double peak spaced symmetrically about the electric field axis (Fig. 4). For this window position (the first set of dashed lines in Fig. 2), the peaks correspond to ions from wave packets localized about axes near $\pm 45°$ from the direction of the ionizing field. Most of the ions from wave packets lying closer to the direction of the electric field axis (0°) arrived before the boxcar window was open, and those further from the axis than 45°, after it was closed. The solid line indicates the theoretical prediction for such a window position and the agreement is excellent. The asymmetry in the peak heights results from the "handedness" of the wave packet. This is, the wave packet is made up of eigenstates that have only positive values of m (the Zeeman quantum number). For a classical model, this corresponds to the handedness of the orbital motion (e.g., clockwise or counterclockwise). An even later time window position (the second set of dashed lines in Fig. 2), splits the peaks further and again we find good agreement with theory (Fig. 5). From these results, the wave packet is found to be $20° \pm 5°$ wide (FWHM), which agrees with the theoretical prediction for these experimental conditions [Fig. 1(a)].

In summary, we have excited and observed an angularly localized wave packet. This wave packet is nearly a minimum-uncertainty state, and it follows a classical trajectory determined by the potential due to the core polarization. And further, the behavior of this wave packet remains classical under the influence of an ionizing field. It should be noted that the precession and dispersion of the wave packet were too slow to be observed by this experiment. This is not surprising since they are driven by a small potential due to the quantum defect of sodium. In fact, if this wave packet were formed in hydrogen, which has no quantum defect, the precession and dispersion would not occur. The wave packet would remain intact, with a fixed orientation in space, until an incoherent process (collisions, spontaneous emission) destroyed the coherence. Also, the results of this experiment suggest that it should be possible to form a wave packet localized in all dimensions, whose motion would correspond to an electron moving in a Kepler orbit. Work in this direction, both theoretical and experimental, is under way.

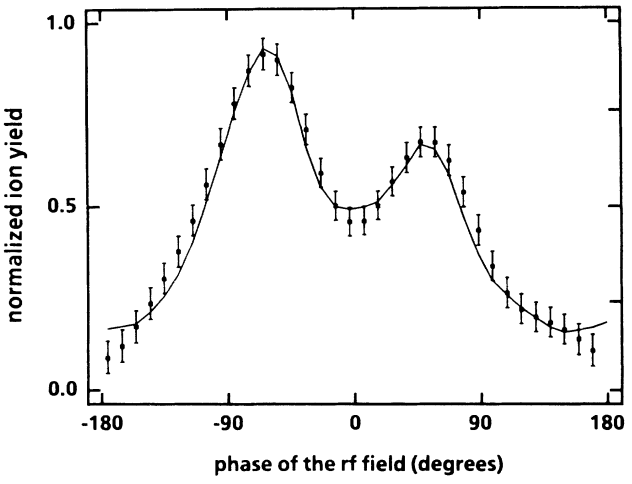

FIG. 4. The ion yield from the angularly localized wave packet as a function of the direction in which it is localized. The window of the boxcar (width = 100 nsec) was delayed by 0.7 μsec from the front edge of the ionization signal. The origin of the x axis (0°) corresponds to the direction of the ionizing electric field. The solid line indicates the results of the classical analysis of the process.

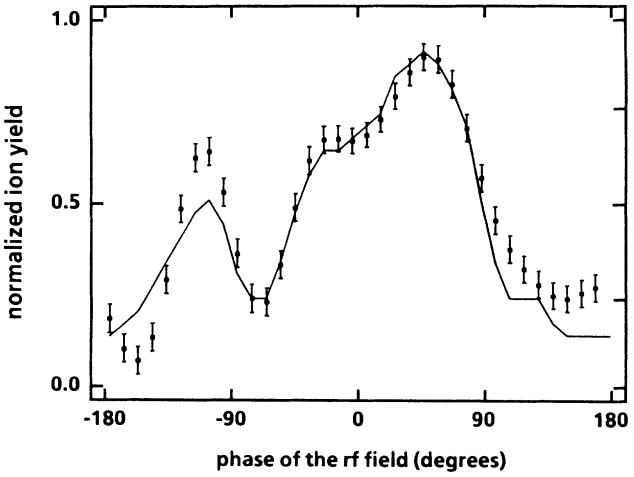

FIG. 5. Same as Fig. 4, but the window (width 100 nsec) was delayed by 1.5 μsec.

This work was supported, in part, by the U.S. Army Research Office and the Joint Services Optics Program.

[1]Jonathan Parker and C. R. Stroud, Jr., Phys. Rev. Lett. **56**, 716 (1986).

[2]G. Alber, H. Ritsch, and P. Zoller, Phys. Rev. A **34**, 1058 (1986).

[3]Jonathan Parker and C. R. Stroud, Jr., Phys. Scr. **T12**, 70 (1986).

[4]J. A. Yeazell and C. R. Stroud, Jr., Phys. Rev. A **35**, 2806 (1987).

[5]W. A. Henle, H. Ritsch, and P. Zoller, Phys. Rev. A **36**, 683 (1987).

[6]E. Schrödinger, Natürwissenschaften **28**, 664 (1926).

[7]M. Perelomov, Commun. Math. Phys. **26**, 222 (1972).

[8]M. M. Nieto and L. M. Simmons, Jr., Phys. Rev. D **20**, 1321 (1979).

[9]M. M. Nieto, Phys. Rev. D **22**, 391 (1980).

[10]Christopher C. Gerry, Phys. Rev. A **33**, 6 (1986).

[11]R. G. Hulet, E. S. Hilfer, and D. Kleppner, Phys. Rev. Lett. **55**, 2137 (1985).

[12]J. G. Leopold and I. C. Percival, Phys. Rev. Lett. **41**, 944 (1978), and J. Phys. B **12**, 709 (1979).

[13]D. A. Jones, J. G. Leopold, and I. C. Percival, J. Phys. B **13**, 31 (1980).

[14]R. V. Jensen, Phys Rev. A **30**, 386 (1984), and Phys. Rev. Lett. **54**, 2057 (1985).

[15]J. G. Leopold and D. Richards, J. Phys. B **18**, 3369 (1985).

[16]J. N. Bardsley, B. Sundaram, L. A. Pinnaduwage, and J. E. Bayfield, Phys. Rev. Lett. **56**, 1007 (1986).

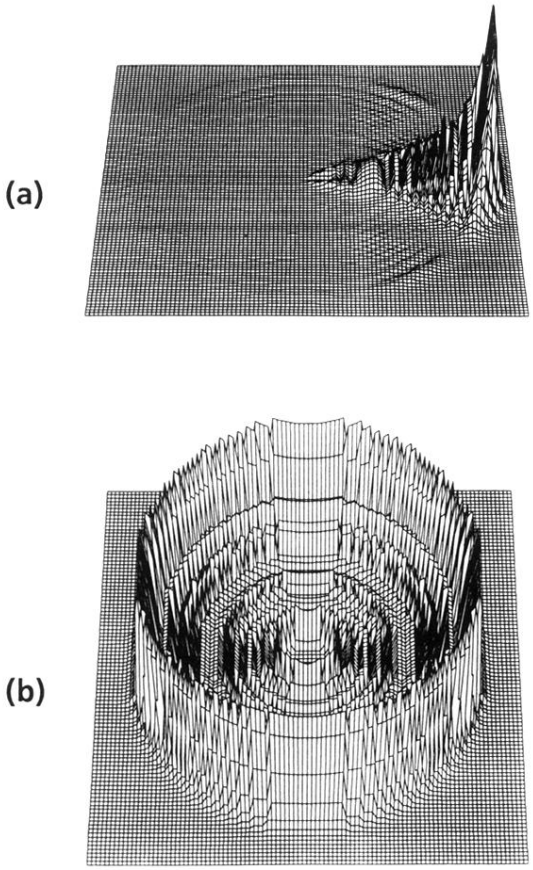

FIG. 1. (a) The probability distribution of the angularly localized wave packet, in the x-y plane, in the form of a 3D plot. Since the wave packet is formed from high-angular-momentum states ($n=50$, $29<l<37$, $m=l$), the probability of the wave packet being found outside of the x-y plane is small. The orientation of the wave packet is along the direction of the rf field vector. The peak of the distribution occurs at 5000 Bohr radii. The parameters used in the numerical model agree with the experimental conditions. (b) The probability distribution of an eigenstate ($n=50$, $l=32$, $m=32$) for comparison.